

AECL-5804

**ATOMIC ENERGY
OF CANADA LIMITED**



**L'ÉNERGIE ATOMIQUE
DU CANADA LIMITÉE**

**EXPERIMENTAL STUDIES ON FLOW-INDUCED VIBRATION
TO SUPPORT STEAM GENERATOR DESIGN**

**PART III: Vibration of Small Tube Bundles in
Liquid and Two-phase Cross-Flow**

by

M.J. PETTIGREW and D.J. GORMAN

**Paper presented at the International Symposium on Vibration Problems
in Industry 10-12 April 1973, Keswick, England**

Chalk River Nuclear Laboratories

Chalk River, Ontario

June 1977


ATOMIC ENERGY OF CANADA LIMITED

EXPERIMENTAL STUDIES ON FLOW-INDUCED VIBRATION
TO SUPPORT STEAM GENERATOR DESIGN

PART III: Vibration of Small Tube Bundles
in Liquid and Two-phase Cross-
Flow

by

M.J. Pettigrew, D.J. Gorman

Paper presented at 
the International Symposium on Vibration Problems in Industry
10-12 April 1973, Keswick, England

Chalk River Nuclear Laboratories
Chalk River, Ontario K0J 1J0
June 1977

AECL-5804

Etudes expérimentales sur la vibration engendrée par l'écoulement
pour faciliter la conception des générateurs de vapeur*

Partie III: Vibration de petits faisceaux de tubes dans un
écoulement transversal liquide et biphasé

par

M.J. Pettigrew et D.J. Gorman

Résumé

Des expériences de vibration ont été effectuées sur de petits faisceaux de tubes pour configurations de réseau triangulaires et carrées dans un écoulement liquide et biphasé (air-eau). Les effets de la vitesse de l'écoulement, de la qualité de la vapeur, de l'orientation du réseau, de l'emplacement des tubes et de la fréquence des tubes, ont été étudiés. La réponse des tubes à l'excitation aléatoire due à la turbulence et l'instabilité fluidélastique ont été observés aussi bien dans l'écoulement transversal liquide que dans le biphasé.

La réponse à la vibration des tubes est mise en corrélation avec une puissance de la vitesse d'écoulement. L'exposant de vitesse se trouve entre 1.5 et 2.6 pour l'écoulement liquide et est près de 1.0 pour l'écoulement biphasé lorsque la vapeur a une qualité constante. Pour une vitesse donnée d'écoulement, l'amplitude de la vibration atteint un maximum lorsque la qualité de la vapeur est approximativement 15%. Les seuils d'instabilité fluidélastique sont mis en corrélation avec la vitesse d'écoulement sans dimension V/fd et l'amortissement sans dimension $m\delta/\rho d^2$ pour l'écoulement liquide et pour le biphasé.

Les critères d'instabilité fluidélastique et les caractéristiques de la fonction de forçage aléatoire sont dérivés de ce travail. Cette information peut être employée dans l'analyse des vibrations des composants d'échangeurs de chaleur du type enveloppe-et-tubes.

Partie I: Vibration d'un cylindre chauffé dans un écoulement axial biphasé, M.J. Pettigrew et D.J. Gorman, L'Energie Atomique du Canada, Limitée, rapport AECL-4514, 1973.

Partie II: Vibration de tube engendrée par l'écoulement liquide transversal dans la région d'entrée d'un générateur de vapeur, M.J. Pettigrew, J.L. Platten et Y. Sylvestre, L'Energie Atomique du Canada, Limitée, rapport AECL-4515, 1973.

* Communication présentée au Symposium international sur les problèmes de vibration dans l'industrie tenu du 10 au 12 avril 1973 à Keswick, Angleterre.

L'Energie Atomique du Canada, Limitée
Laboratoires Nucléaires de Chalk River
Chalk River, Ontario, KOJ 1J0
Juin 1977

ATOMIC ENERGY OF CANADA LIMITED

EXPERIMENTAL STUDIES ON FLOW-INDUCED VIBRATION
TO SUPPORT STEAM GENERATOR DESIGN*

PART III: Vibration of Small Tube Bundles
in Liquid and Two-Phase Cross-
Flow

by

M.J. Pettigrew, D.J. Gorman

ABSTRACT

Vibration experiments were done on small tube bundles of triangular and square lattice configurations in both liquid and two-phase (air-water) cross-flow. The effects of flow velocity, simulated steam quality, lattice orientation, tube location and tube frequency were explored. Tube response to random flow turbulence excitation and fluidelastic instability were observed in both liquid and two-phase cross-flow.

The tube vibration response is related to a power of the flow velocity. The velocity exponent is between 1.5 and 2.6 for liquid flow and nearly 1.0 for two-phase flow at constant steam quality. For a given flow velocity the vibration amplitude reaches a maximum at a steam quality of roughly 15%. Fluidelastic instability thresholds are related to dimensionless flow velocity V/fd and dimensionless damping $m\delta/\rho d^2$ for both liquid and two-phase cross-flow.

Fluidelastic instability criteria and random forcing function characterizations are derived from this work. This information may be used in the vibration analysis of shell-and-tube heat exchanger components.

Part I: Vibration of a heated cylinder in two-phase axial flow, M.J. Pettigrew and D.J. Gorman, Atomic Energy of Canada Limited, report AECL-4514, 1973.

Part II: Tube vibration induced by liquid cross-flow in the entrance region of a steam generator, M.J. Pettigrew, J.L. Platten, and Y. Sylvestre, Atomic Energy of Canada Limited, report AECL-4515, 1973.

* Paper presented at the International Symposium on Vibration Problems in Industry, 10-12 April, 1973, Keswick, England.

EXPERIMENTAL STUDIES ON FLOW-INDUCED VIBRATION
TO SUPPORT STEAM GENERATOR DESIGN

PART III: Vibration of Small Tube Bundles
in Liquid and Two-phase Cross-
Flow

INTRODUCTION

Two-phase steam/water cross-flow exists in the "U" bend tube region of vertical recirculating type steam generators¹. The void fraction and consequently the mean flow velocity are relatively high. The "U" bend tube region should be analysed from a flow-induced vibration point of view to avoid potential problems. This requires an understanding of the vibration behaviour of a tube bundle in two-phase cross-flow.

Several researchers^{2,3,4,5,6,7,8} have reported data on periodic wake shedding frequencies (in the form of Strouhal numbers $S = fd/v$) in single-phase (gas or liquid) cross-flow in various tube arrays. Some of this data is summarized in reference 1. Chen⁹ has presented limited information on the magnitude of the fluctuating lift coefficient C_L associated with periodic wake shedding in tube bundles.

Other possible vibration excitation mechanisms are fluidelastic instabilities and forced response to random pressure fluctuations due to flow turbulence. Connors¹⁰ and Roberts¹¹ have done some work on fluidelastic type instabilities in tube arrays in single phase flow. Random excitation is often mentioned; however, little data is available on the statistical parameters such as spatial correlations and spectral density functions necessary to define it.

To the knowledge of the authors no information has been reported in the literature on any of the above possible vibration excitation mechanisms for two-phase cross-flow in tube bundles.

This note presents the results of an exploratory vibration experiment on small tube bundles in two-phase (air/water) cross-flow. Tube bundles of both triangular and square tube lattice configuration were tested. The tube bundles were subjected to various mass fluxes and simulated steam qualities. Some tests were done in liquid cross-flow for comparison. The results show that fluidelastic type instabilities are also possible in two-phase flow.

2. EXPERIMENTAL

2.1 Flow Conditions and Test Apparatus

At the top of the steam generators of the typical CANDU-PHW* nuclear stations of Pickering and Bruce, the flow conditions are respectively 12.5 and 20% steam quality, and 340 (0.25×10^6) and 217 $\text{kg}/(\text{m}^2\text{s})$ (0.16×10^6 $\text{lb}/(\text{h}.\text{ft}^2)$) free stream mass flux (no tubes) at a pressure of approximately 4.35 MPa (630 psia). The above mass fluxes are based on the cross-sectional area of the steam generator tube bundle shroud and are used as reference values for the present investigation. Actual mass fluxes should be similar or somewhat smaller as the steam-water mixture flows radially out in the hemispherically shaped "U" bend region. The complex geometry of this region makes flow velocity calculations difficult.

The experiments were conducted in an air/water test loop to simulate two-phase flow steam/water mixtures. Volumetric flows of air and water were set equal to those of steam and water. Thus flow velocities and void fractions were duplicated. Coincidentally at 20% steam quality the mean density of the air/water mixture is only 4% greater than that of the simulated steam/water.

Several small tube bundles were installed in the cross-tube of the test section shown on Figure 1. Homogenized air/water mixtures were introduced at the inlet of the test section by means of a carefully designed mixer located immediately upstream. To simulate realistic mass fluxes with the available capacity of the loop, the flow area was limited to 38.7 cm^2 (6 in^2). The inlet was streamlined in a nearly rectangular shape to provide flow of 50.8 mm (2 in.) uniform width across the diameter and at the center of the tube bundles.

Tests were also done in liquid flow for comparison. The mixer was removed during those tests. The Reynolds number based on the gap velocity and the tube diameter varied between 10^4 and 10^5 .

Triangular and square tube bundle configurations both of 19 mm (0.75 in.) pitch were tested. The tubes were supported in flanges at both ends of the cross-tube with "O" ring seals. The holes in the flanges were tapered towards the "O" ring to ensure pinned end conditions. The tube bundle could be rotated at the end flanges. Thus both normal and parallel triangular lattice, and both normal and rotated square lattice could be tested by simply rotating the respective tube bundles.

* CANDU-PHW (CANAda Deuterium Uranium - Pressurized Heavy Water).

The tube length between "O" ring supports was either 0.914 (36) or 1.22 m (48 in.). This simulated tube frequencies in the range of interest (i.e., fundamental mode natural frequencies are 17 and 30 Hz). All tubes were stainless steel type 304 12.9 mm (0.50 in.) OD and 0.76 mm (0.030 in.) wall thickness except for the instrumented tubes of the short bundle which were Inconel 600, 12.9 mm (0.51 in.) OD and 1.12 mm (0.044 in.) wall. The tubes were filled with water to simulate in-service conditions. The tubes were completely immersed in water over their entire length in liquid flow tests and over all but the flow path (≈ 50.8 mm) in two-phase tests.

2.2 Instrumentation and Data Analysis

One long and two short tubes were each instrumented with weldable strain gauges. The gauges were installed as close as possible to the centre of the tubes without being in the flow stream. The instrumented tubes could be installed at any location within the tube bundle.

We used the same analysis equipment as that described in Part II of this paper^{1,2}. Analyses of the signals showed that the tube response could be described as narrow-band random. The tubes vibrated mostly in their fundamental natural mode. The observed frequencies were 17 and 30 Hz from the long and short bundle respectively. We did not expect nor observe second mode response since the flow impinged at a nodal point of that mode.

Very low amplitude third mode response was noticed particularly with the long tube bundle but was not considered further in the analysis. Selected frequency analyses are on Figure 2.

The mean square of the dynamic strain signals was obtained by squaring and averaging by integration over a period of time $T = 60$ s. The operation was repeated several times to ensure stationary conditions. Prior to squaring, the signals were fed through a 5 to 100 Hz band-pass filter to eliminate DC shifts and high frequency signal noise.

3. RESULTS AND DISCUSSION

3.1 General

In simulated two-phase flow, the effect of mass flux at constant steam quality for the various tube bundle configuration and length is shown on Figure 3. Figure 4 shows the effect of simulated steam quality, the mass flux being kept constant. The vibration response vs flow velocity in liquid flow is

presented in Figure 5. Figure 6 shows the variation in tube vibration response in terms of the tube location within the bundle.

The vibration amplitude at midspan is deduced from the dynamic strain measurements ϵ assuming fundamental natural mode response of a simply supported beam (i.e., $y(x,t) = y(\ell/2,t) \sin\pi x/\ell$). The so-called instantaneous "resultant" vibration amplitude at midspan $y_R(\ell/2,t)$ is the vectorial sum of the amplitude in the direction parallel to the flow $y_P(\ell/2,t)$ and the amplitude in the direction normal to it $y_N(\ell/2,t)$, and is the maximum amplitude of the tube at a given time t . It may be shown that the RMS resultant amplitude used in the presentation of the results is expressed by:

$$\overline{y_R^2}(\ell/2,t) = \overline{y_P^2}(\ell/2,t) + \overline{y_N^2}(\ell/2,t) \quad (1)$$

and is obtained simply from the addition of the mean square response in each direction. The numbers in brackets on the figures are the ratios of the mean square amplitude in the direction of the flow over same normal to it

$$\text{(i.e., } \overline{y_P^2} / \overline{y_N^2}\text{)}.$$

It is an indication of the preferred direction of vibration.

The mass fluxes and flow velocities are normalized to take into account the effect of the irregular flow paths between the tube bundle and the test section walls. They are stated in terms of free stream or approach mass fluxes and flow velocities. The mass fluxes are expressed in terms of the simulated steam/water mass fluxes. Thus the flow velocities are the actual flow velocities.

3.2 Vibration Response in Liquid Flow

There are no indications of resonance peaks due to periodic wake shedding in the amplitude vs flow velocity curves of Figure 5. This is not surprising since the tubes are only excited over a small area resulting in very low amplitudes at the velocities likely to promote periodic wake shedding resonance, i.e., 0.2 to 0.6 m/s (0.7 to 1.8 ft/s) based on Chen's data⁸.

The tube response is generally directly related to a power of the velocity. This is indicative of broad-band random excitation. The velocity exponent is 2.6 and 1.9 for the short and long bundle respectively. The vibration responses of the normal and parallel triangular tube bundles were practically the same whereas the amplitudes of the normal square bundle were roughly 1.5 times larger for the same flow velocities. The behaviour of the rotated square lattice is somewhat different and remains unexplained. As shown on Figure 6 vibration of upstream tubes is not significantly higher than that of center tubes in liquid flow.

The amplitude of the long tube bundle increases very rapidly at a given flow velocity. This is attributed to a fluid-elastic type instability of the same nature as that described by Connors¹⁰. This is discussed further in Section 3.4. The amplitude increases further with velocity until it is limited by the presence of adjacent tubes. Then considerable rattling noise could be heard.

The preferred direction of vibration in liquid flow is normal to the flow direction except under instability conditions. This suggests dominant random fluctuating lift forces. No instabilities were observed with the short bundle probably because the critical velocities were not reached. However the change of preferred vibration direction at the highest amplitudes for both the normal square and the parallel triangular configurations may indicate the threshold of instability.

3.3 Vibration Response in Two-Phase Flow

The vibration response of the tube bundle in two-phase cross-flow at constant steam quality (mostly 20%) is roughly proportional to the mass flux except at low mass fluxes (see Figure 3). The apparent discrepancy there is due to the sluggish nature of the flow at low mass flux. That is the two-phase mixture is not so well homogenized and large slugs of water and large air bubbles are formed between the mixer and the tube bundle. Ignoring the low flow data, mass flux exponents between 0.9 and 1.3 would approximately fit the observed response. That these components are lower than 2, which would have been expected from energy considerations, may be explained by changes in flow regime or in the structure of the two-phase flow mixture. This mass-flux relationship is similar to that observed in Part I of this paper¹³ for axial two-phase flow.

The flow velocities calculated for periodic wake shedding resonance in liquid flow correspond to very low mass fluxes in two-phase flow. At such low mass fluxes, the excitation due to the more sluggish flow regime would be much stronger than periodic wake shedding assuming that it does at all exist in two-phase flow. There is no evidence of periodic excitation at the higher mass fluxes either. Thus the vibration excitation in two-phase flow appears broad-band random in nature.

The vibration amplitude of the long tube bundle increases sharply at higher mass fluxes. This is attributed to fluid-elastic type instabilities (see Section 3.4).

In two-phase flow, upstream tubes vibrate most (see Figure 6). Also tubes near the wall of the test section tend to vibrate more than interior tubes (see Tube No. 5 vs No. 1 on Figure 6b).

The parallel triangle and normal square bundles vibrate least, the rotated square most, and the normal triangle bundle somewhat less. The opposite is observed in liquid flow. The preferred direction of vibration is in the flow direction which is also the opposite. Thus fluctuating lift forces are not dominant and periodic lift forces probably not significant. The above shows that the vibration behaviour in two-phase flow is considerably different than in single phase flow.

The effect of simulated steam quality is shown on Figure 4. The vibration amplitude is maximum at approximately 15% quality. This trend may be attributed to flow regime or flow structure changes and is strongest for the normal triangular lattice configuration. Somewhat similar results were obtained in two-phase axial flow, see reference 13.

3.4 Fluidelastic Instability Analysis

The instability thresholds taken from Figures 3 and 5 are presented on Figure 7 together with similar results from Connors¹⁰ and Gorman et al¹⁴. Fluidelastic instabilities are expressed in terms of dimensionless velocity V/fd and dimensionless mass or damping $m\delta/\rho d^2$. The density ρ in two-phase flow is taken as the homogeneous density of the mixture. The logarithmic decrement values of damping δ were obtained from tests and are stated in Figure 7. The damping was practically linear over the range of amplitude of interest. The mass per unit length m includes the water inside the tubes and the hydrodynamic mass due to the inertia of the water surrounding the tubes. The latter is taken as equivalent to the mass of water displaced by the tubes.

We used a so-called "normalized gap velocity" V_{gn} for the dimensionless velocity term. V_{gn} is the gap velocity normalized so that, distributed uniformly along the entire length of the tube span, it has the same effect as the gap velocity V_g over the portion of the tube subjected to flow. Connor's expression¹⁰ for the critical velocity for fluid-elastic instability of tubes subjected to uniform flow over their entire length is essentially:

$$V_g / fd = V_{gn} / fd = K \sqrt{m\delta / \rho d^2} \quad (2)$$

It is shown in Appendix 1 that for tubes subjected to uniform flow V_g from x_1 to x_2 along the length of the tube span, the expression becomes:

$$V_g / fd = K \sqrt{\delta / [\rho d^2 \int_{x_1}^{x_2} \phi^2(x) dx]} \quad (3)$$

where $\phi(x)$ is the normalized mode shape such that

$$\int_0^l m\phi(x)^2 dx = 1.$$

From equations (2) and (3) we get:

$$V_{gn} = V_g \sqrt{m \int_{x_1}^{x_2} \phi^2(x) dx} \quad (4)$$

which is the expression used to calculate V_{gn} in Figure 7. Thus V_{gn} equals $0.33 V_g$ and $0.29 V_g$ for the 0.914 m (36 in.) and 1.22 m (48 in.) tube bundles respectively.

Regardless of the tube bundle orientation, we define the gap velocity as

$$V_g = V_\alpha p / (p-d) \quad (5)$$

where p and d are respectively the tube lattice pitch and the tube diameter and V_α is the free stream velocity. The gap velocity defined above is the true gap velocity for both normal triangular and normal square configurations. It is not for the parallel triangular and rotated square configurations. For the latter the so-defined gap velocity is only an indication

of the maximum flow velocity and is related to the density of the tube bundle configuration. This definition of the velocity has two advantages. Firstly, it enables the designer to compare directly the two principal orientations of a tube bundle from a fluidelastic vibration viewpoint. All flow directions are usually possible in one or another region of actual heat exchangers. Secondly, the fluidelastic phenomena appears related to the maximum velocity in the tube bundle rather than the free stream velocity.

We find that for our tube bundles a coefficient of around 6.6 is more appropriate to define instability than 9.9 as suggested by Connors for his single row of tubes (see Figure 7). Note that the same fluidelastic instability criterion appears to apply for both liquid and two-phase flow.

3.5 Random Excitation Analysis

As discussed earlier, the dominant vibration excitation mechanism at flow velocities below that required for fluid-elastic instability is random flow turbulence. Appendix 2 shows that, providing some simplifying assumptions are made, the power spectral density $S_{(g)}$ of the random turbulence excitation may be inferred from the response as follows:

$$S_{(g)} = \overline{y^2} (\ell/2) [4\pi^3 f_1^3 \zeta m^2 \ell^2] \quad (6)$$

where $\zeta = \delta/2\pi$ is the damping ratio. The most important assumption made is that the random force field be homogeneous and spatially correlated. In reality this is not quite correct. However the random forces should be much better correlated over the 50.8 mm (2.0 in.) width of our test section than over the much larger flow areas of actual heat exchangers. Thus vibration response analyses based on the so-derived random excitation forces would yield conservative results when applied to heat exchanger design providing the forces are also assumed to be correlated in the analyses.

Figures 8 and 9 show the vibration response data obtained for triangular configurations below the threshold velocity for fluidelastic instability. The lines on these figures are the upper limits of vibration response normalized to the flow velocity squared in liquid flow and to the mass flux G in two-phase flow. The normalized power spectral density of the random excitation is obtained from these upper limit lines using Equation (6). The results presented as the normalized power spectral density function are shown on Figures 10 and 11.

Although the above deductions are somewhat contentious, they nevertheless give the designer an idea of the magnitude of the random flow turbulence forces. Interestingly, similar deductions from data obtained in a quite different experiment¹² yielded results which are in the same range as shown on Figure 10.

The power spectral density function of the random flow turbulence forces generally decreases with frequency for both liquid and two-phase flow as expected. This may be partly explained by the reduced spatial correlation of high frequency components.

Figure 11 shows values at simulated steam qualities other than 20%. These were derived using Figure 4 to establish the steam quality relationship. Again the values are based on upper limit curves. The data point used are shown on Figure 4.

3.6 Significance of the Results to the Designer

The above results have the following practical significance to the designer of steam generators and heat exchangers:

- 1) Both fluidelastic instability and response to random flow turbulence should be considered as vibration excitation mechanisms in two-phase flow.
- 2) To allow for a realistic safety margin, a fluidelastic instability coefficient of 3.3 is recommended for vibration analyses of steam generators.
- 3) A triangular tube lattice should be preferable from a flow-induced vibration point of view if the flow is in all directions as is the case in steam generators. The triangular lattice has the additional advantage that it allows for more tubes per unit volume for a given pitch.
- 4) Large tube-free volumes should be avoided in steam generators. These would allow the formation of large slugs of water or large plugs of steam which could cause large vibration amplitudes of nearby tubes when hit by this slug/plug flow.

4. CONCLUDING REMARKS

The results of an exploratory vibration experiment on small tube bundles in two-phase (air/water) and liquid cross-flow show that:

- 1) Fluidelastic instability appears possible in two-phase flow as well as in liquid flow. The same instability criterion seems to apply for both. An instability coefficient of around 6.6 fits the results best.
- 2) Other than fluidelastic instability, vibration response to random flow turbulence is the dominant vibration excitation mechanism. Tube vibration response to random flow turbulence is related to a power of the flow velocity. The velocity exponent is between 1.5 and 2.6 for liquid flow and roughly 1.0 for two-phase flow.
- 3) In liquid flow, the vibration responses of the normal and parallel triangular tube bundles are roughly the same whereas that of the normal square bundle is 50% larger. In two-phase flow, the parallel triangle and normal square bundles vibrate least, whereas the rotated square vibrates most.
- 4) In liquid flow, the vibration amplitude was generally larger in the direction normal to the flow than in the flow direction. In two-phase flow the opposite was observed.
- 5) Vibration amplitudes are maximum at roughly 15% steam quality.
- 6) In two-phase flow upstream tubes vibrate most.

5. ACKNOWLEDGEMENT

The authors are grateful to G.A.W. Hewitt for his technical assistance.

6. REFERENCES

- 1) SCHNEIDER, W., PETTIGREW, M.J., HODGE, R.I.,
"Vibration Analysis in the Design of Steam Generating
Equipment for the Bruce Nuclear Power Station",
Paper No. 523, International Symposium on Vibration
Problems in Industry, Keswick, England, (1973),
also Atomic Energy of Canada Limited, Report AECL-4478.
- 2) KONIG, A. & GREGORIG, R., "Ein Schwingungskriterium
eines quer Angelströmten Rohres," Chem. Ing. Techn. 40,
13, 645-650, 1968.
- 3) OWEN, P.R., "Buffeting Excitation of Boiler Tube
Vibration", J. Mech. Eng. Sci. 7, 4, 431-439, 1965.
- 4) CHEN, Y.N., "Ursache und Vermeidung Rauchgasseitiger
Schwingungserscheinungen in Kesselanlagen infolge
Brenngasdrallinstabilität und Karman-Wirbelstrassen"
VGB 51, 2, 113-123, 1971.
- 5) HILL, R.S., "Aerodynamic Sound in Tube Banks", Proc.
Phys. Soc. 79, 225-227, 1962.
- 6) PUTNAM, A.A., "Flow-induced Noise and Vibration in
Heat Exchangers", ASME 64-WA/HT-21, 1964.
- 7) BORGES, A.R.J., "Vortex Shedding Frequencies of the
Flow Through Two-row Banks of Tubes", J. Mech. Eng.
Sci., 11, 5, 498-502, 1969.
- 8) CHEN, Y.N., "Flow-Induced Vibration and Noise in Tube-
Bank Heat Exchangers due to Von Karman Streets"
ASME Paper 67-VIBR-48, 1967.
- 9) CHEN, Y.N., "Fluctuating Lift Forces of the Karman
Vortex Streets on Single Circular Cylinders and in
Tube Bundles, Part 3 - Lift Forces in Tube Bundles",
ASME Publication, 71-Vibr-13, Jour. Eng. for Industry. 1971.
- 10) CONNORS, H.J., "Fluidelastic Vibration of Tube Arrays
Excited by Cross Flow", Paper presented at Winter Annual
Meeting, American Society of Mechanical Engineers,
New York, December 1970.
- 11) ROBERTS, B.W., "Low Frequency, Aeroelastic Vibrations
in a Cascade of Circular Cylinders", Mech. Engrg. Sci.
Monograph No. 4, Sept. 1966.

- 12) PETTIGREW, M.J., PLATTEN, J.L., SYLVESTRE, Y., "Experimental Studies on Flow Induced Vibration to Support Steam Generator Design; Part II: Tube Vibration Induced by Liquid Cross-Flow in the Entrance Region of a Steam Generator", Paper No. 424, International Symposium on Vibration Problems in Industry, Keswick, U.K. (1973), also Atomic Energy of Canada Limited, Report AECL-4515.
- 13) PETTIGREW, M.J., GORMAN D.J., "Experimental Studies on Flow Induced Vibration to Support Steam Generator Design; Part I: Vibration of a Heated Cylinder in Two-Phase Axial Flow", Paper No. 424, International Symposium on Vibration Problems in Industry, Keswick, U.K. (1973), also Atomic Energy of Canada Limited, Report AECL-4514.
- 14) MIRZA, S., GORMAN D.J., "Experimental and Analytical Correlation of Local Driving Forces and Tube Response in Liquid Flow Induced Vibration of Heat Exchangers", Paper F 6/5, Intl. Conf. on Structural Mechanics in Reactor Technology, Berlin, September 1973.
- 15) THOMSON, W.T., "Vibration Theory and Applications", Prentice-Hall, Englewood Cliffs, N.J., 1965.
- 16) MEIROVITCH, L., "Analytical Methods in Vibration", Macmillan Company, N.Y., 1967.
- 17) CRANDALL, S.H., MARK, W.D., "Random Vibration in Mechanical Systems", Academic Press, N.Y., 1963.

APPENDIX 1

FLUIDELASTIC INSTABILITY ANALYSIS

The relationship for fluidelastic instability of tube bundles subjected to non-uniform flow is derived in this appendix. The derivation is a generalization of Connors' formulation¹⁰. Fluidelastic instabilities are possible in a tube bundle when the interaction between the motions of the individual tubes is such that it results in fluid force components that are both proportional to tube displacements and in-phase with tube velocities. Instability occurs when during one vibration cycle the energy absorbed from the fluid forces exceeds the energy dissipated by damping.

In a tube bundle subjected to the non-uniform flow velocity $V_g(x)$, the vibration response $y(x,t)$ at time t and point x along the length ℓ of any tube may be generally expressed by:

$$y(x,t) = Y_r(x) \sin \omega_r t \quad (1.1)$$

where $Y_r(x)$ is the maximum amplitude of the r^{th} mode, and ω_r its natural frequency. It is reasonable to assume harmonic motion and little coupling between the modes since damping is light.

The fluid force component per unit length $P_f(x,t)$ that is in-phase with the tube vibration velocity is conveniently formulated as

$$P_f(x,t) = (ky(x,t+\pi/2)/d) \rho V_g^2(x)d/2 \quad (1.2)$$

where d is the tube diameter, ρ is the fluid density, k is a fluid-force/tube-motion proportionality constant and $t + \pi/2$ indicates the phase. The energy input E_f due to the fluid forces over the length of the tube for one

vibration cycle may be expressed with the help of Equation (1.1) and (1.2) as:

$$E_f = (\kappa\rho\omega_r/2) \int_0^l \int_0^{2\pi/\omega_r} v_g^2(x) Y_r^2(x) \cos^2(\omega_r t) dt dx \quad (1.3)$$

or

$$E_f = (\pi\kappa\rho/2) \int_0^l v_g^2(x) Y_r^2(x) dx \quad (1.4)$$

The damping force $P_c(x,t)$ per unit length is:

$$P_c(x,t) = c \, dy(x,t)/dt \quad (1.5)$$

where c is the coefficient of damping per unit length.

The energy dissipated by damping E_c during one vibration cycle, assuming that damping occurs along the whole length of the tube, is given by:

$$E_c = (c \omega_r^2) \int_0^l \int_0^{2\pi/\omega_r} Y_r^2(x) \cos^2(\omega_r t) dt dx \quad (1.6)$$

or

$$E_c = \pi c \omega_r \int_0^l Y_r^2(x) dx \quad (1.7)$$

Fluidelastic instability occurs when $E_f \geq E_c$. Thus the threshold velocity for fluidelastic instability may be formulated from Equation (1.4) and (1.7):

$$\pi c \omega_r \int_0^{\ell} Y_r^2(x) dx = (\pi k \rho / 2) \int_0^{\ell} V_g^2(x) Y_r^2(x) dx \quad (1.8)$$

Since $Y_r(x)$ is directly proportional to the natural mode $\phi_r(x)$ and if $\phi_r(x)$ is normalized so that

$$\int_0^{\ell} m \phi_r^2(x) dx = 1 \quad (1.9)$$

Equation (1.8) becomes

$$c \omega_r / m = (k \rho / 2) \int_0^{\ell} V_g^2(x) \phi_r^2(x) dx \quad (1.10)$$

where m is the mass per unit length. Defining $K = \sqrt{8\pi/k}$ and $V_g(x)$ in terms of a flow velocity distribution function $\psi(x)$ so that

$$V_g(x) = V_g \psi(x) \quad (1.11)$$

and rearranging, we get:

$$V_g / f_r d = K \sqrt{c / [2 f_r d^2 m \rho \int_0^{\ell} \psi^2(x) \phi_r^2(x) dx]} \quad (1.12)$$

This equation may be expressed in terms of the logarithmic decrement of damping δ , since $c = 2\delta m f_r$, hence

$$v_g / f_r d = K \sqrt{\delta / [\rho d^2 \int_0^l \phi_r^2(x) \psi^2(x) dx]} \quad (1.13)$$

If the tubes are subjected to a uniform flow V_g from x_1 to x_2 along their length and to no flow elsewhere, $\psi(x) = 1$ for $x_1 < x < x_2$ and $\psi(x) = 0$ for $x_1 > x > x_2$; thus Equation (1.13) becomes:

$$v_g / f_r d = K \sqrt{\delta / [\rho d^2 \int_{x_1}^{x_2} \phi_r^2(x) dx]} \quad (1.14)$$

For the special case where the flow is uniform over the whole length of the tubes $\psi(x) = 1$ and

$$\int_{x_1}^{x_2} \phi_r^2(x) dx = \int_0^l \phi_r^2(x) dx = 1/m \quad (1.15)$$

Replacing in Equation (1.13), it reduces to Connor's expression, that is:

$$v_g / f_r d = K \sqrt{\delta m / \rho d^2} \quad (1.16)$$

APPENDIX 2

The expressions relating tube response to random excitation due to flow turbulence are formulated in this appendix.

It may be shown with the assistance of References 15, 16 and 17 that the mean square response $\overline{y^2}(x)$ of a uni-dimensional continuous uniform cylindrical structure to distributed random forces $g(x,t)$ may be expressed by:

$$\overline{y^2}(x) = \sum_r \sum_s \frac{\phi_r(x) \phi_s(x)}{16\pi^4 f_r^2 f_s^2} \int_0^\alpha |H_r(f)| |H_s(f)| \cos[\theta_r(f) - \theta_s(f)]$$

$$\int_0^l \int_0^l \phi_r(x) \phi_s(x') R(x, x', f) dx dx' df \quad (2.1)$$

where: 1) the spatial correlation density functions $R(x, x', f)$ is defined by

$$R(x, x', f) = 2 \int_{-\alpha}^{\alpha} \left[\lim_{T \rightarrow \infty} \frac{1}{2T} \int_{-T}^T g(x, t) g(x', t+t) dt \right] e^{-j(2\pi f)t} dt \quad (2.2)$$

2) the frequency response function is

$$H_r(f) = \frac{1}{\left(1 - \frac{f^2}{f_r^2}\right) + 2j\zeta_r \frac{f}{f_r}} \quad (2.3)$$

ζ_r is the damping ratio at the r^{th} mode and θ_r is the argument of $H_r(f)$.

3) $\phi_r(x)$ and $\phi_s(x)$ represent the normal mode of vibration of the structure for the r^{th} and s^{th} mode, and

4) x and x' are points on the structure and τ is a difference in time t .

For the above derivation we assume that the damping is small and that it does not introduce coupling between modes to justify modal analysis. The natural modes are normalized so that

$$\int_0^l m \phi_r^2(x) dx = 1 \quad (2.4)$$

where m is the mass per unit length.

Using Equation 2.1 we can calculate the response of a tube knowing the spatial correlation density function of the distributed random forces. Conversely, knowing the response, we may obtain some knowledge of the random forces. Consider now the fundamental mode only of a lightly damped simply supported cylinder (i.e., $\phi_1(x) = (2/lm)^{1/2} \sin(\pi x/l)$). This is essentially the case of the experiment discussed in this report. Since we have little information on the statistical properties of the distributed random forces we assume:

1) that the random force field is homogeneous, the power spectral density function of the force $S(g)$ is independent of location, i.e.,

$$R(x, x', f) = R'(x, x') S(g) \quad (2.5)$$

2) that both $S(g)$ and the spatial correlation $R'(x, x')$ are fairly independent of frequency near the fundamental frequency of the cylinder, such that the space and frequency terms in Equation 3 may be separated and that:

$$\int_0^\alpha |H_r(f)| |H_s(f)| \cos \left[\theta_r(f) - \theta_s(f) \right] df = \pi f_1 / 4\tau \quad (2.6)$$

and

3) that the random forces $g(x, t)$ are completely correlated and constant over the tube region exposed to flow and nil elsewhere, i.e.,

$$R'(x, x') = 1 \text{ for } x_1 < x < x_2 \quad (2.7)$$

and

$$R'(x, x') = 0 \text{ for } 0 < x < x_1 \text{ and } x_2 < x < \ell \quad (2.8)$$

Substituting Equations (2.4), (2.5), (2.6), (2.7) and (2.8) in (2.1) and rearranging we get for $x = \ell/2$ (i.e., midspan):

$$\overline{y^2}(\ell/2) = \frac{S(g)}{32\pi^3 f_1^3 \zeta_m \ell} \int_{x_1}^{x_2} \int_{x_1}^{x_2} \phi_1(x) \phi_1(x') dx dx' \quad (2.9)$$

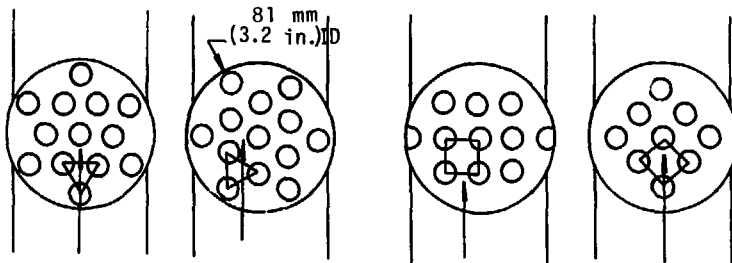
In the experiment $x_1 = \ell/2 - 1$, $x_2 = \ell/2 + 1$, and near $\ell/2$, $\phi_1(x) = (2/\ell m)^{1/2}$ thus

$$\overline{y^2}(\ell/2) = \frac{S(g)}{4\pi^3 f_1^3 \zeta m^2 \ell^2} \quad (2.10)$$

or

$$S(g) = \overline{y^2}(\ell/2) \left[4\pi^3 f_1^3 \zeta m^2 \ell^2 \right] \quad (2.11)$$

which may be used to estimate the power spectral density function $S(g)$ of the excitation from the response $\overline{y^2}(\ell/2)$.



NORMAL
TRIANGULAR

PARALLEL

FLOW

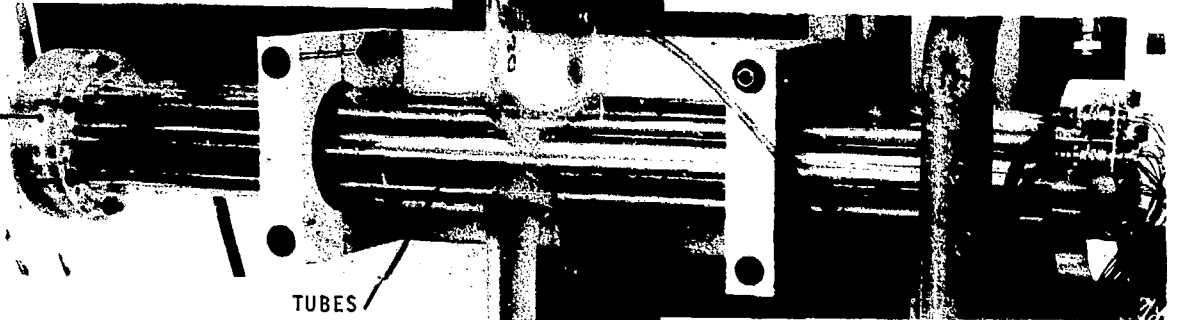
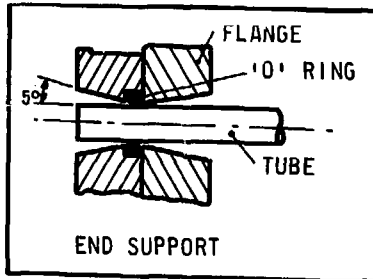
NORMAL
SQUARE

ROTATED

TUBE BUNDLE LATTICE CONFIGURATIONS

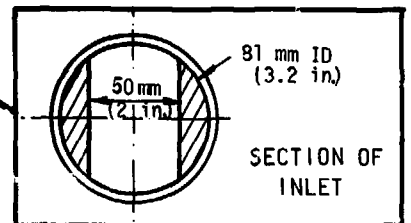


AIR/WATER FLOW

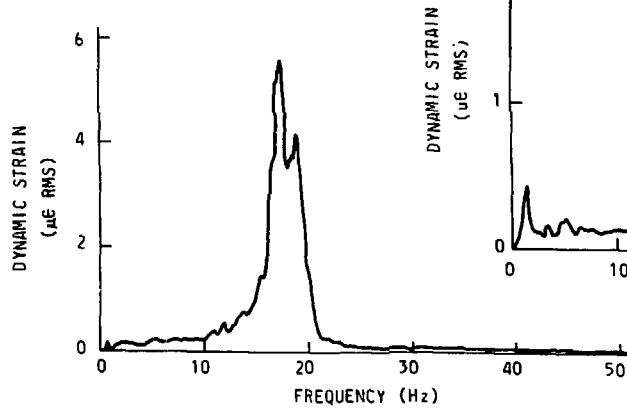


OUTLET

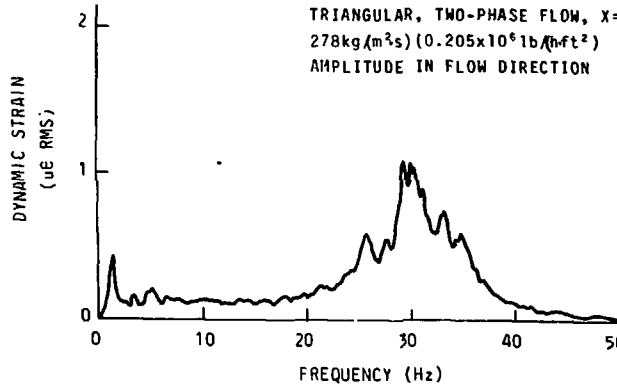
FIGURE 1: TEST SECTION, DETAILS AND TUBE BUNDLE LATTICE CONFIGURATIONS.



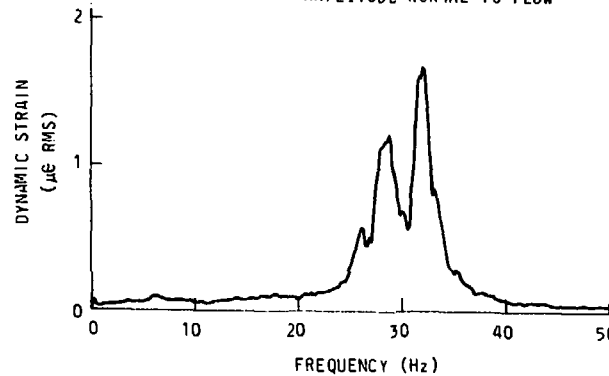
a) 1.22 m (48 in.) CENTRAL TUBE, NORMAL
 TRIANGULAR, TWO-PHASE FLOW, $X=20\%$
 $340\text{kg}/(\text{m}^2\text{s})$ ($0.287 \times 10^6 \text{lb}/(\text{hft}^2)$)
 AMPLITUDE IN FLOW DIRECTION



c) 0.914 m (36 in.), CENTRAL TUBE, NORMAL
 TRIANGULAR, TWO-PHASE FLOW, $X=20\%$,
 $278\text{kg}/(\text{m}^2\text{s})$ ($0.205 \times 10^6 \text{lb}/(\text{hft}^2)$)
 AMPLITUDE IN FLOW DIRECTION



d) 0.914 m (36 in.), CENTRAL TUBE, PARALLEL
 TRIANGULAR, TWO-PHASE FLOW, $X=20\%$
 $478\text{kg}/(\text{m}^2\text{s})$ ($0.308 \times 10^6 \text{lb}/(\text{hft}^2)$)
 AMPLITUDE NORMAL TO FLOW



b) 1.22 m (48 in.), CENTRAL TUBE, PARALLEL
 TRIANGULAR, LIQUID FLOW, $\text{VEL}=1.74 \text{ m/s}$
 (5.72 ft/s)
 AMPLITUDE IN FLOW DIRECTION

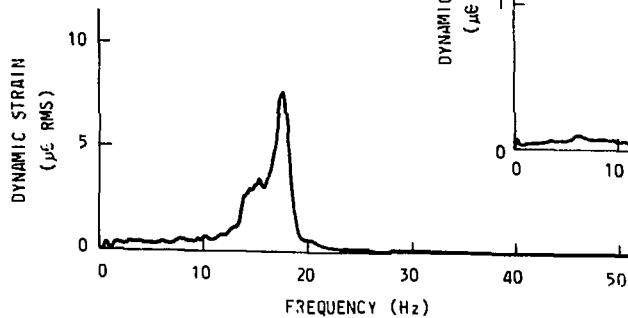


FIGURE 2: TYPICAL FREQUENCY SPECTRA.

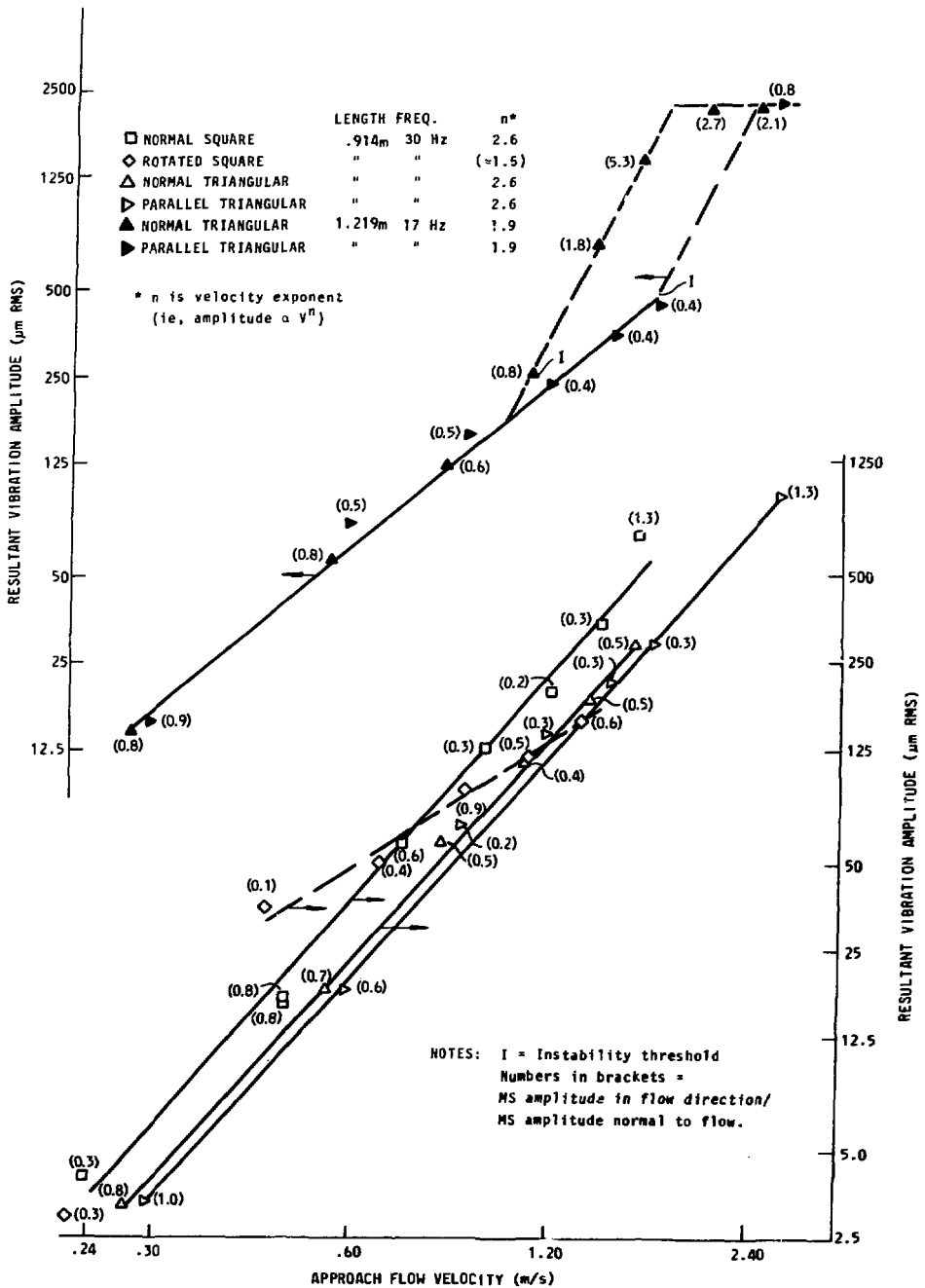
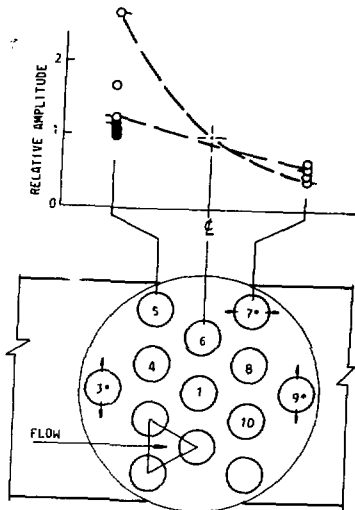
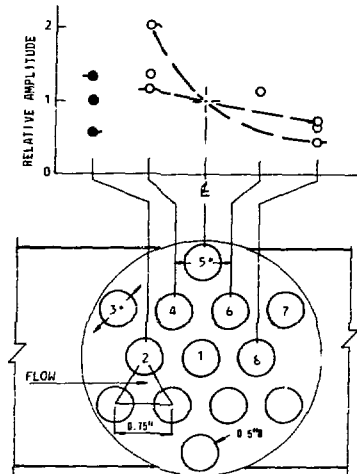


FIGURE 5 EFFECT OF FLOW VELOCITY ON VIBRATION AMPLITUDE OF CENTRAL TUBE IN LIQUID FLOW



TUBE LOCATION	TWO-PHASE FLOW: $x=20\%$ SIMULATED MASS FLUX [10^6 lb/h.ft^2]		
	[0.102]	[0.205]	[0.287]
1	1.96(1.2)	4.80(1.6)	6.42(2.6)
3	1.12*	3.02*	6.78*
4	2.45(3.0)	8.00(2.5)	17.30(1.1)
6		4.32(2.3)	
7		2.52*	
9		0.80*	
10	1.20(2.1)	2.25(3.4)	2.62(2.1)
	LIQUID FLOW: FLOW VELOCITY [ft/s]		
	[1.83]	[3.65]	[5.34]
1	0.73(0.7)	4.49(0.4)	11.58(0.5)
4	0.87(0.6)	4.97(0.2)	11.81(0.3)

a) NORMAL TRIANGULAR



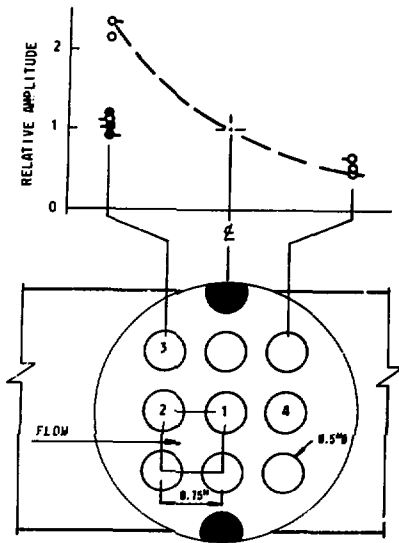
TUBE LOCATION	TWO-PHASE FLOW: $x=20\%$ SIMULATED MASS FLUX [10^6 lb/h.ft^2]		
	[0.110]	[0.220]	[0.308]
1	1.81(0.8)	2.89(2.2)	4.62(2.2)
3	1.08*	3.43*	8.05*
4	2.07(1.0)	3.88(0.7)	9.33(1.2)
5		4.46*	
6		3.37(1.6)	
8	1.27(1.3)	1.87(3.1)	2.10(2.4)
	LIQUID FLOW: FLOW VELOCITY [ft/s]		
	[2.94]	[5.72]	[8.80]
1	2.71(0.2)	11.67(0.3)	37.90(1.3)
2	3.56(0.2)	11.80(0.3)	21.30(0.3)

b) PARALLEL TRIANGULAR

NOTES: Numbers in tables are resultant vibration amplitudes (10^{-3} in RMS)
 Numbers with asterisks are vibration amplitudes in direction shown only.
 Numbers in brackets = MS amplitude in direction of flow/MS amplitude normal to flow.

SI Unit Conversion Factors: $10^6 \text{ lb/(h.ft}^2) = 1357 \text{ kg/(sm}^2)$
 $1.0 \text{ ft/s} = 0.305 \text{ m/s}$; 10^{-3} in RMS = 25.4 $\mu\text{m RMS}$.

FIGURE 6a and b: Location Dependency of Vibration Response (For 30 Hz Tubes).

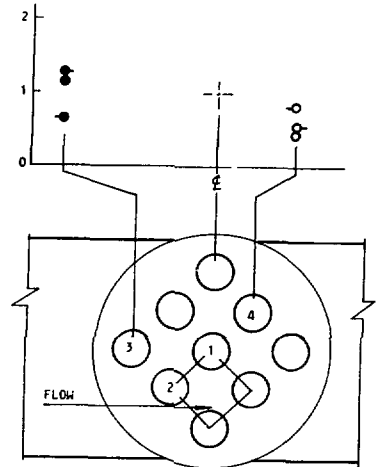


TWO-PHASE FLOW: $x=20\%$

TUBE LOCATION	SIMULATED MASS FLUX [10^6 lb/h.ft^2]		
	[0.088]	[0.177]	[0.266]
1	2.14(1.3)	2.81(0.8)	3.63(1.4)
2	2.33(1.6)	6.03(2.2)	8.41(3.0)
3	2.51(4.0)	6.16(5.9)	7.37(3.8)
4	1.39(0.8)	1.45(0.9)	1.79(1.1)

TUBE LOCATION	LIQUID FLOW: FLOW VELOCITY [ft/s]		
	[2.36]	[3.94]	[5.74]
1	2.37(0.6)	7.89(0.2)	27.56(1.3)
2	2.64(0.2)	9.28(0.3)	25.20(0.2)

c) NORMAL SQUARE



TWO-PHASE FLOW: $x=20\%$

TUBE LOCATION	SIMULATED MASS FLUX [10^6 lb/h.ft^2]		
	[0.083]	[0.166]	[0.249]
1	1.77(2.5)	4.54(0.8)	6.68(1.5)
4	1.46(1.2)	1.97(1.4)	3.00(2.2)

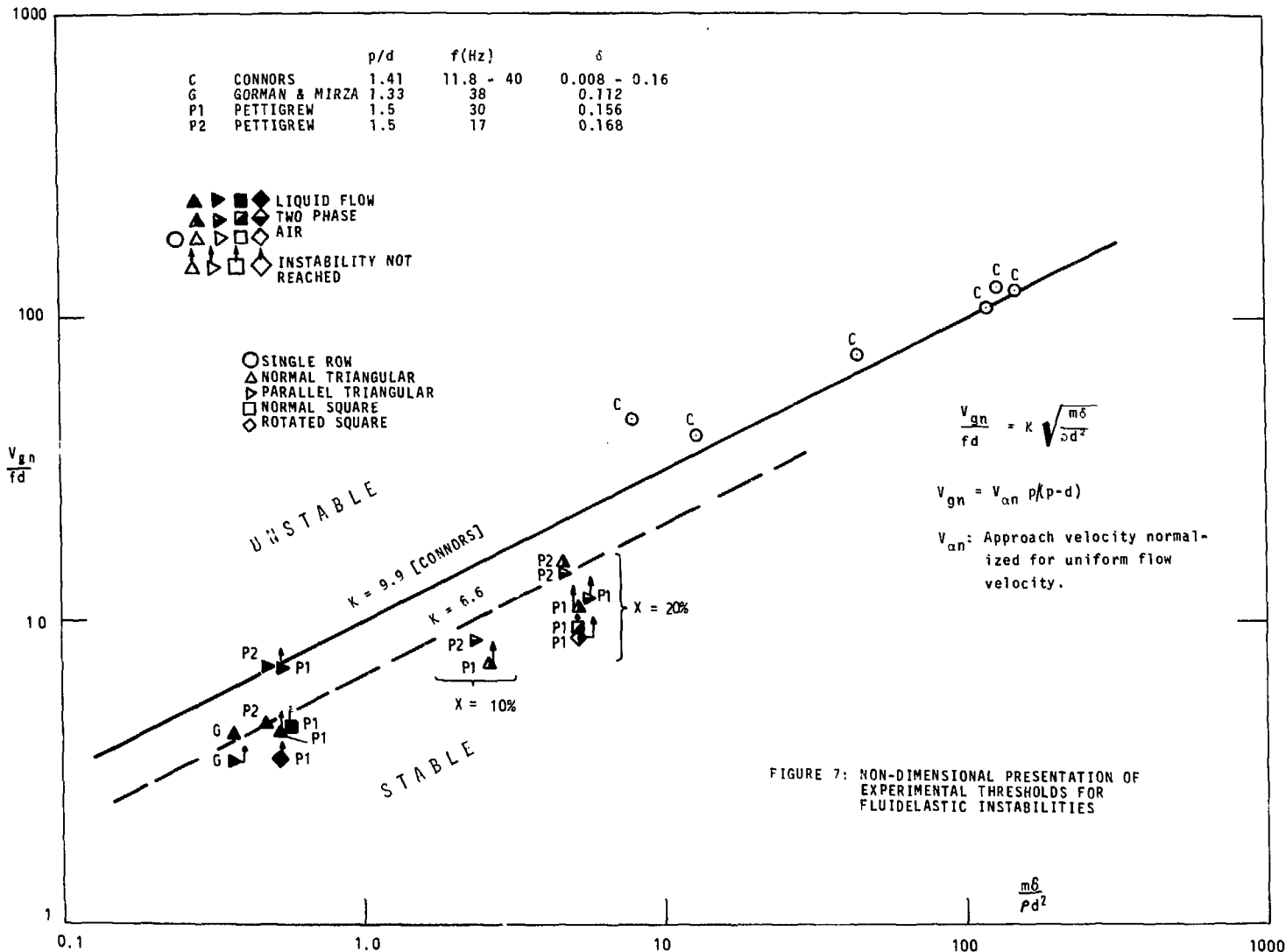
TUBE LOCATION	LIQUID FLOW: FLOW VELOCITY [ft/s]		
	[1.48]	[2.95]	[4.43]
1	1.42(0.1)	3.61(0.4)	6.35(0.6)
3	0.89(0.5)	4.24(0.4)	8.07(0.5)

d) ROTATED SQUARE

NOTES: Numbers in tables are resultant vibration amplitudes (10^{-3} in RMS). Numbers with asterisks are vibration amplitudes in direction shown only. Numbers in brackets = MS amplitude in direction of flow/MS amplitude normal to flow.

SI Unit Conversion Factors: $10^6 \text{ lb/(h.ft}^2) = 1357 \text{ kg/(sm}^2)$;
 $1.0 \text{ ft/s} = 0.305 \text{ m/s}$; $10^{-3} \text{ in RMS} = 25.4 \text{ } \mu\text{m RMS}$.

FIGURE 6c and d: Location Dependency of Vibration Response (For 30 Hz Tubes).



	LENGTH	FREQ.
△ NORMAL TRIANGULAR	.914 m	30 Hz
▽ PARALLEL TRIANGULAR	"	"
▲ NORMAL TRIANGULAR	1.219 m	17 Hz
▼ PARALLEL TRIANGULAR	"	"

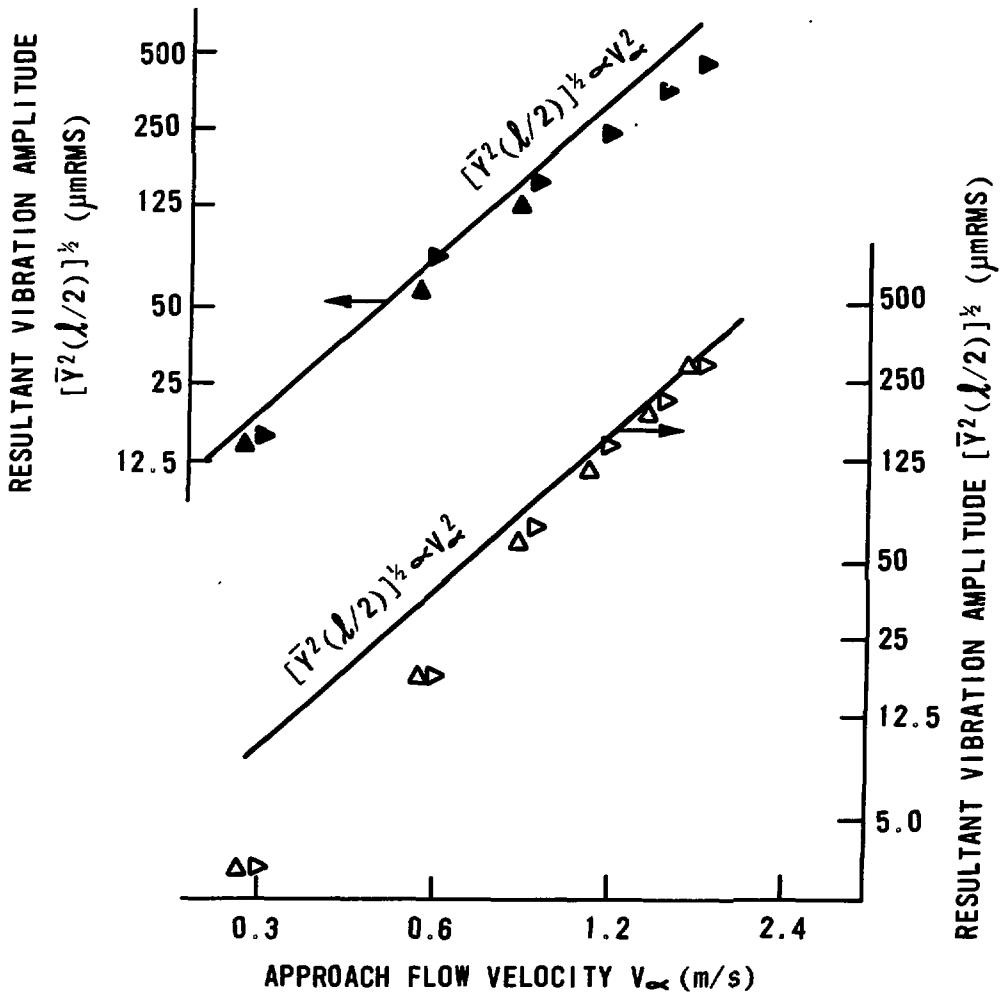


FIGURE 8: Effect of Flow Velocity on Vibration Amplitude of Central Tube in Liquid Flow (Upper Limit of Vibration Response Normalized to Velocity Squared).

1.219 m TUBES (17 Hz)

▲ NORMAL TRIANGULAR
▶ PARALLEL "

.914 m TUBES (30 Hz)

▲ NORMAL TRIANGULAR
▶ PARALLEL "

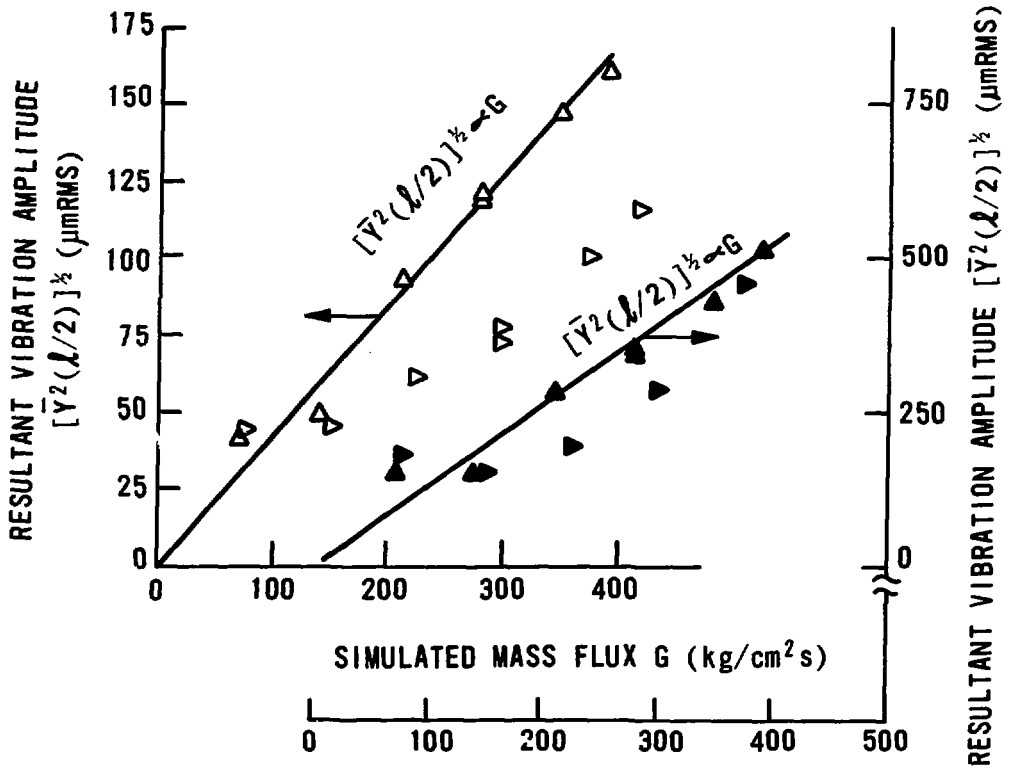


FIGURE 9: Effect of Mass Flux on Vibration Amplitude of Central Tube in Two-Phase Flow at 20% Simulated Steam Quality (Upper Limit of Vibration Response Normalized to Mass Flux).

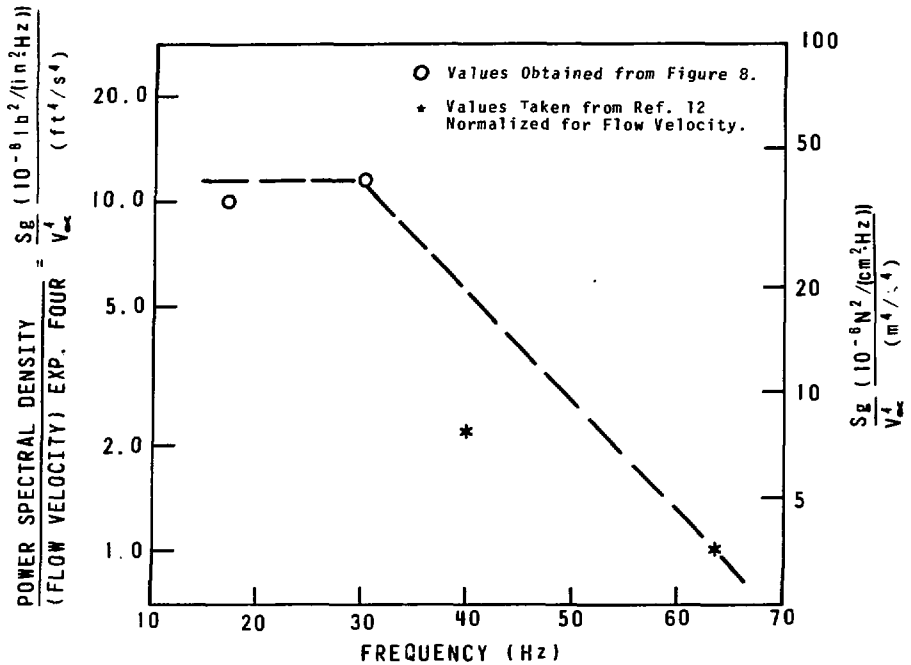


FIGURE 10: Deduced Normalized Power Spectral Density of Random Turbulence Excitation in Liquid Flow.

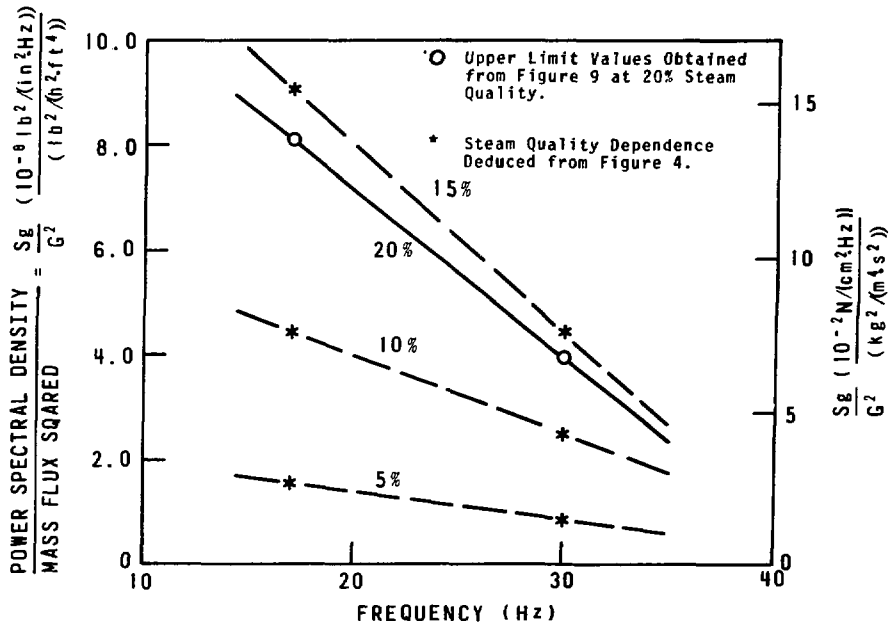


FIGURE 11: Deduced Normalized Power Spectral Density of Random Turbulence Excitation in Two-Phase Flow.

The International Standard Serial Number

ISSN 0067-0367

has been assigned to this series of reports.

**To identify individual documents in the series
we have assigned an AECL-number.**

**Please refer to the AECL-number when
requesting additional copies of this document
from**

**Scientific Document Distribution Office
Atomic Energy of Canada Limited
Chalk River, Ontario, Canada**

K0J 1J0

Price \$3.00 per copy

1077-77